

# Topological Insights into Black Hole Thermodynamics: Non-Extensive Entropy in CFT framework

Mohammad Ali S. Afshar,<sup>1,\*</sup> Mohammad Reza Alipour,<sup>2,1,†</sup> Saeed Noori Gashti,<sup>2,‡</sup> and Jafar Sadeghi<sup>1,§</sup>

<sup>1</sup>*Department of Physics, Faculty of Basic Sciences, University of Mazandaran  
P. O. Box 47416-95447, Babolsar, Iran*

<sup>2</sup>*School of Physics, Damghan University, P. O. Box 3671641167, Damghan, Iran*  
(Dated: January 3, 2025)

In this paper, We conducted an in-depth investigation into the thermodynamic topology of Einstein-Gauss-Bonnet black holes within the framework of Conformal Field Theory (CFT), considering the implications of non-extensive entropy formulations. Our study reveals that the parameter  $\lambda$  (Rényi entropy) plays a crucial role in the phase behavior of black holes. Specifically, when  $\lambda$  is below the critical value ( $C$ ), it has a negligible impact on the phase behavior. However, when  $\lambda$  exceeds the critical value, it significantly alters the phase transition outcomes. Determining the most physically representative values of  $\lambda$  will require experimental validation, but this parameter flexibility allows researchers to better explain black hole phase transitions under varying physical conditions. Furthermore, the parameters  $\alpha$  and  $\beta$  affect the phase structure and topological charge for the Sharma-Mittal entropy. Only in the case of  $C > C_c$  and in the condition of  $\alpha \approx \beta$  will we have a first-order phase transition with topological charge  $+1$ . Additionally, for the loop quantum gravity non-extensive entropy as the parameter  $q$  approaches 1, the classification of topological charges changes. We observe configurations with one and three topological charges with respect to critical value  $C$ , resulting in a total topological charge  $W = +1$ , and configurations with two topological charges ( $\omega = +1, -1$ ), leading to a total topological charge  $W = 0$ . These findings provide new insights into the complex phase behavior and topological characteristics of black holes in the context of CFT and non-extensive entropy formulations.

Keywords: Einstein-Gauss-Bonnet black holes; CFT; Non-extensive entropy

## CONTENTS

I. Introduction	2
II. Gauss-Bonnet-AdS black hole	3
A. CFT thermodynamics for GB-AdS black hole with $d = 5$	3
III. Thermodynamic topology	5
IV. Non-extensive Entropy	6
V. Thermodynamic topology and the Rényi entropy	7
A. $C = 0.15 < C_c$	7
B. $C = 2.5 > C_c$	8
VI. Thermodynamic topology and Sharma-Mittal entropy	10
A. $C = 0.15 < C_c$	10
B. $C = 2.5 > C_c$	11
VII. Thermodynamic topology within LQG	11
A. Case I: $C = 0.15 < C_c$	13
B. Case II: $C = 2.5 > C_c$	14
VIII. Conclusions	14
References	14

\* m.a.s.afshar@gmail.com

† mr.alipour@stu.umz.ac.ir

‡ saeed.noorigashti@stu.umz.ac.ir; saeed.noorigashti70@gmail.com

§ pouriya@ipm.ir

## I. INTRODUCTION

The AdS/CFT correspondence is a powerful concept in theoretical physics that proposes a duality between two types of physical theories: gravitational theories in Anti-de Sitter (AdS) space and conformal field theories (CFT) defined on the boundary. This correspondence can open numerous avenues for diverse and varied studies in cosmological physics. The AdS/CFT correspondence provides a rich framework for exploring the connections between quantum field theories, thermal dynamics, and gravity. In this context, the thermodynamic properties of black holes in AdS space (such as temperature and entropy) have direct analogs in the thermodynamics of CFT, deepening our understanding of the fundamental laws of the universe. For instance, black holes residing in AdS space exhibit Hawking radiation (thermal particles emitted from black holes), which can be understood based on the dual degrees of freedom in CFT. The emitted radiation corresponds to excitations in the boundary theory, indicating a profound connection between black hole dynamics and field theory [1–4]. Conversely, the CFT living on the boundary of AdS space has its own thermodynamic characteristics. In many cases, especially at high temperatures, this CFT can be described using a statistical ensemble, where states are thermally populated according to their energy. Consequently, the CFT partition function can be computed via the Euclidean path integral on the boundary. The free energy of the CFT can be related to the gravitational action computed in the bulk AdS space. Establishing such bridges allows for the calculation of various thermodynamic observables, such as Helmholtz free energy, Gibbs free energy, and entropy, from black hole solutions in AdS and the corresponding CFT [5]. Additionally, the rich phase structure in AdS black holes enables the analysis of phase transitions between different thermodynamic states, linking them to the structural properties of the corresponding CFT. In summary, when a black hole forms in AdS, the corresponding thermal state in the CFT can be identified.

One of the most intriguing and significant aspects of classical thermodynamics, which typically contains vital information about the behavior of the sample under study, is the examination of phase transitions. Phase transitions are traditionally analyzed by examining the behavior of temperature-dependent plots of the Gibbs free energy. In a first-order phase transition, this results in the appearance of a swallowtail form, while in a second-order phase transition, it leads to a smoothly curved plot. The use of this traditional method to study the thermodynamics of black holes has been explored in various researches [6–8]. However, it must be acknowledged that due to the complexity of black hole field equations, these studies, particularly for the swallowtail form, have encountered significant difficulties.

In 2017, Cunha and colleagues [9, 10] proposed using the extrema of the rewritten effective potential, combined with the concept of winding, to study the topology of photon rings and photon spheres in flat black holes. This method was subsequently extended by Wei to asymptotically AdS and dS black holes [11], leading to numerous studies based on this approach and relative validation of the method [12–19]. Since the overall method was based on the structure of the scalar quantity of energy, it suggested that scalar functions exhibiting similar behavior could benefit from this general method for study. Accordingly, Wei extended this method to thermodynamics and, for the first time, applied it to the study of critical points of a sample based on the behavior of the temperature function [20]. This preliminary work primarily focused on finding the critical points of black holes as a thermodynamic sample, and did not provide much information about phase transitions. Subsequently, Wei and colleagues extended this method to the Helmholtz free energy [21], which in initial studies indicated very interesting information about black hole phase transitions. Following this innovation, numerous studies were conducted in both forms, particularly the free energy method, demonstrating its effectiveness [22–61]. In fact, the F method in these studies showed that it could effectively represent the phase transition behavior of black holes.

Given this background, it is essential to clearly state our motivation and objective in this study. In the method of using the Helmholtz free energy ( $F$ ) to study phase transitions, whether in the traditional form or the topological method, we consider a thermodynamic parameter as the target parameter for classifying the phase transition space. This is based on the first law of thermodynamics and the canonical perspective of the sample. We then examine the phase behavior of the sample around the critical points of this parameter. Typically, this target parameter is temperature or pressure. In this paper, we aim to shift the role of the target parameter to the central charge and investigate the phase behavior of the sample around the critical points of this parameter, to see if this difference will lead to a different view of the sample's topological phase transition. Also, since the definition of free energy is intertwined with the concept of entropy, we will not limit our study to the usual Bekenstein-Hawking entropy. Instead, we will incorporate super statistical entropies to examine and compare the impact of additional parameters of these new entropies on phase transitions. Regarding the use of super statistical entropies in this research, it should be noted that although comprehensive studies on the mutual effects of super statistics and gravitational structures have not yet been systematically conducted, and most studies are scattered, these studies show that the need for non-standard and super statistical descriptions is one of the essential requirements for the development of studies. [62, 63]. Traditional statistical mechanics typically relies on invoking equilibrium distributions (such as the Boltzmann distribution). However, many real-world systems are inherently non-equilibrium, influenced by varying external conditions or local interactions that can lead to significant fluctuations in energy, temperature, or other thermodynamic variables. Super statistics provides a framework for describing such systems by incorporating local statistical variations. Therefore, it seems essential to pay more attention to the contribution and impact of super statistical perspectives in studies of systems with complex behaviors, such as black holes.

With respect to all the above statements, we arrange the paper as follows. In section II, we briefly review the model. In Sections III and IV we study the overview of the thermodynamic topology method and introduction of nonextensive entropy such as Rényi, Sharma-Mittal, and loop quantum gravity. In Section V, VI, VII we will study and analyze using the different superstatistical entropies for the introduced model. Finally, we have conclusions which are summarized in Section VIII.

## II. GAUSS-BONNET-ADS BLACK HOLE

The Gauss-Bonnet-AdS black hole is studied in detail. The action for the  $d$ -dimensional Einstein-Maxwell theory is presented, incorporating the Gauss-Bonnet term along with a negative cosmological constant [64–67],

$$S = \frac{1}{16\pi G} \int d^d x \sqrt{-g} \left[ R - 2\Lambda + \alpha_{GB} (R_{\mu\nu\sigma\rho} R^{\mu\nu\sigma\rho} + R^2 - 4R_{\mu\nu} R^{\mu\nu}) - 4\pi G F_{\mu\nu} F^{\mu\nu} \right]. \quad (1)$$

The equation incorporates the electromagnetic field tensor, represented as  $F_{\mu\nu} = \partial_\mu A_\nu - \partial_\nu A_\mu$ , alongside the Gauss-Bonnet coupling constant  $\alpha_{GB}$ , Newton's constant  $G$ , and the cosmological constant  $\Lambda$ . In string theory, the Gauss-Bonnet coupling constant is positive with dimensions of  $(length)^2$ . Here, we focus on a spherical horizon topology, which corresponds to  $k = 1$ . As a result, the metric can be expressed in the following form,

$$ds^2 = -f(r)dt^2 + f^{-1}(r)dr^2 + r^2(d\theta^2 + \sin^2\theta d\phi^2 + \cos^2\theta d\Omega_{d-4}^2), \quad (2)$$

and,

$$f(r) = 1 + \frac{r^2}{2\beta_0} \left[ 1 - \left( 1 + \frac{64\pi\beta_0 GM}{(d-2)\Sigma r^{d-1}} - \frac{8G\beta_0 Q^2}{(d-2)(d-3)r^{2(d-2)}} - \frac{4\beta_0}{\ell^2} \right)^{\frac{1}{2}} \right], \quad (3)$$

The quantities  $\Sigma$ ,  $Q$ , and  $M$  denote the area of the  $d-2$  dimensional unit sphere, the electric charge, and the black hole's mass, respectively. Furthermore,  $\beta_0 = (d-4)(d-3)\alpha_{GB}$ . By solving the equation  $f(r_+) = 0$  and using the relation  $T = \frac{f'(r_+)}{4\pi}$ , the mass and temperature of the black hole can be calculated [64–67],

$$M = \frac{\Sigma(d-2)r_+^{d-3}}{16\pi G r_+^2 \ell^2} (r_+^2 \ell^2 + \beta \ell^2 + r_+^4) + \frac{\Sigma Q^2}{8\pi(d-3)r_+^{d-3}}, \quad (4)$$

and,

$$T = \frac{(d-1)(d-2)r_+^{2(d-2)} + (d-2)(d-3)\ell^2 r_+^{2(d-3)} + (d-5)(d-2)\beta_0 r_+^{2(d-4)} - 2GQ^2}{4\pi r_+ (r_+^2 + 2\beta_0)\ell^2 (d-2)r_+^{2(d-4)}}, \quad (5)$$

The entropy of the black hole can also be represented as [26],

$$S = \frac{\Sigma r_+^{d-2}}{4G} \left( 1 + \frac{2(d-2)\beta_0}{(d-4)r_+^2} \right). \quad (6)$$

We then analyze the CFT thermodynamic properties of a five-dimensional ( $d = 5$ ) Gauss-Bonnet black hole.

### A. CFT thermodynamics for GB-AdS black hole with $d = 5$

To study the thermodynamics of a charged AdS black hole within the context of CFT, we employ holographic correspondences that link bulk and boundary quantities. In this analysis, the curvature radius of the boundary, denoted as  $R$ , is distinct from the AdS radius  $\ell$  in the bulk. The CFT metric, defined by its conformal scaling invariance, is expressed accordingly [68–70],

$$ds^2 = \omega^2 (-dt^2 + \ell^2 d\Omega_{d-2}^2). \quad (7)$$

The dimensionless conformal factor, denoted as  $\omega$ , is allowed to vary freely, reflecting the conformal symmetry inherent in the boundary theory. In the spherical case,  $d\Omega_{d-2}^2$  represents the metric of a  $(d-2)$ -dimensional sphere, with its volume

denoted by  $\Omega_{d-2} = k$ . It is assumed that  $\omega$  does not depend on the boundary coordinates. Under these assumptions, the volume of the conformal field theory (CFT) is determined accordingly[71, 72],

$$\mathcal{V} = kR^{d-2}, \quad (8)$$

The variable curvature radius of the manifold hosting the CFT is denoted as  $R = \omega\ell$ . Consequently, the variation in the CFT volume  $\mathcal{V}$  remains entirely unaffected by changes in the central charge  $C$ . This central charge exhibits a dual relationship in the framework of Einstein's gravity, as demonstrated in the following equation [71–73],

$$C = \frac{k\ell^{d-2}}{16\pi G}. \quad (9)$$

We keep Newton's constant  $G$  fixed while allowing the bulk curvature radius,  $\ell$ , to vary, thereby altering the central charge  $C$  as outlined in equation (9). The first law of thermodynamic in the CFT case for a five-dimensional GB-AdS black hole and the correspondence between the bulk and boundary values are obtained as follows [73],

$$\delta E = \tilde{T}\delta\tilde{S} + \mu\delta C - p\delta\mathcal{V} + \tilde{\Phi}\delta\tilde{Q} + \tilde{A}\delta\tilde{\beta}_0 \quad (10)$$

$$E = \frac{M}{\omega}, \quad \tilde{S} = S, \quad \tilde{T} = \frac{T}{\omega}, \quad \tilde{\Phi} = \frac{\Phi\sqrt{G}}{\omega\ell}, \quad \tilde{Q} = \frac{Q\ell}{\sqrt{G}}, \quad \tilde{A} = \frac{\mathcal{A}}{\omega\ell}, \quad \tilde{\beta}_0 = \ell\beta_0, \quad (11)$$

$$\begin{aligned} \mu &= \frac{1}{C}(E - \tilde{T}S - \tilde{\Phi}\tilde{Q} - \tilde{A}\tilde{\beta}_0) \\ p &= \frac{E}{3\mathcal{V}}, \quad \mathcal{V} = kR^3 \end{aligned} \quad (12)$$

Where  $\mu$  is the thermodynamic conjugate of the central charge, i.e., the chemical potential,  $\Phi$  is the electric potential, and  $\mathcal{A}$  is the thermodynamic conjugate of the Gauss-Bonnet parameter. Also, equation (11) establishes the correspondence between bulk and boundary quantities. We aim to derive the internal energy formula for the GB black hole in five dimensions within the framework of CFT. For  $d = 5$ , we find that  $\beta_0 = 2\alpha$ . To determine the internal energy formula for the CFT, we define two dimensionless parameters as follows[73],

$$x \equiv \frac{r_+}{\ell} \quad y \equiv \frac{\tilde{\beta}_0}{\ell^3}, \quad (13)$$

Thus, based on equations (4), (6), (9), (11), and (13), we obtain,

$$\begin{aligned} E &= \frac{\Sigma \left( k^2\tilde{Q}^2 + 768\pi^2 C^2 x^6 + 768\pi^2 C^2 x^4 + 768\pi^2 C^2 x^2 y \right)}{256\pi^2 C (k^2\mathcal{V})^{\frac{1}{3}} x^2} \\ \tilde{S} &= \frac{4\pi C \Sigma (x^3 + 6xy)}{k}. \end{aligned} \quad (14)$$

Additionally, we can determine the thermodynamic properties of the CFT,

$$\tilde{T} = \left( \frac{\partial E}{\partial \tilde{S}} \right)_{\tilde{Q}, \mathcal{V}, C, \tilde{\beta}} = \left( \frac{k}{\mathcal{V}} \right)^{\frac{1}{3}} \left( \frac{-k^2\tilde{Q}^2 + 1536\pi^2 C^2 x^6 + 768\pi^2 C^2 x^4}{1536\pi^3 C^2 x^3 (x^2 + 2y)} \right), \quad (15)$$

$$\tilde{\Phi} = \left( \frac{\partial E}{\partial \tilde{Q}} \right)_{\tilde{S}, \mathcal{V}, C, \tilde{\beta}} = \left( \frac{k^4}{\mathcal{V}} \right)^{\frac{1}{3}} \left( \frac{\Sigma \tilde{Q}}{128\pi^2 C x^2} \right), \quad (16)$$

$$p = - \left( \frac{\partial E}{\partial \mathcal{V}} \right)_{\tilde{S}, \tilde{Q}, C, \tilde{\beta}} = \frac{E}{2\mathcal{V}}, \quad (17)$$

$$\mu = \left( \frac{\partial E}{\partial C} \right)_{\tilde{S}, \tilde{Q}, \mathcal{V}, \tilde{\beta}} = \frac{\Sigma \left( -k^2\tilde{Q}^2 + 768\pi^2 C^2 x^6 + 768\pi^2 C^2 x^4 + 768\pi^2 C^2 x^2 y \right)}{256\pi^2 C^2 k^{2/3} \sqrt[3]{\mathcal{V}} x^2}, \quad (18)$$

$$\tilde{A} = \left( \frac{\partial E}{\partial \beta} \right)_{\tilde{S}, \tilde{Q}, \nu, C} = \frac{3C\Sigma y}{\tilde{\beta}^3 \sqrt{k^2 \mathcal{V}}}. \quad (19)$$

Here, equation (17) represent the equation of state in CFT. The concept of a variable Newton's constant is relevant exclusively within the framework of the mixed first law, which modifies the volume term in the black hole phase transition formula. Conversely, the internal energy formula, the boundary first law, and the Euler relation do not require a dynamic Newton's constant. The primary objective is to establish a precise dual correspondence between the bulk and boundary first laws. To resolve the degeneracy between the volume ( $\mathcal{V}$ ) and the central charge ( $C$ ), a dynamic parameter,  $\omega$ , is introduced. These variables are employed to examine the various stages across different thermodynamic ensembles within the dual CFT framework. In CFT thermodynamics, the phase structure of a black hole can be analyzed through the Helmholtz free energy, defined as:

$$\mathcal{F} = E - \tilde{T}\tilde{S}. \quad (20)$$

### III. THERMODYNAMIC TOPOLOGY

Recent advancements have introduced innovative methods for analyzing and identifying critical points and phase transitions in black hole thermodynamics. One notable approach is the topological method, which employs Duan's topological current  $\phi$ -mapping theory to offer a topological perspective on thermodynamics[20, 21]. To examine the thermodynamic properties of black holes, various quantities such as mass and temperature are utilized to describe the generalized free energy. Given the relationship between mass and energy in black holes, the generalized free energy function is expressed as a standard thermodynamic function. The Euclidean time period  $\tau$  and its inverse, the temperature  $T$ , are essential components in this formulation. The generalized free energy is considered on-shell only when  $\tau$  equals the inverse of the Hawking temperature[20, 21]. A vector  $\phi$  is constructed to facilitate this analysis, with components derived from the partial derivatives of the generalized free energy. The direction of this vector is significant, as it points outward at specific angular positions, indicating the ranges for the horizon radius and angular coordinates. Using Duan's  $\phi$ -mapping topological current theory, a topological current can be defined, which is conserved according to Noether's theorem. To determine the topological number, the topological current is reformulated, incorporating the Jacobi tensor. This tensor simplifies to the standard Jacobi form under certain conditions, and the conservation equation reveals that the topological current is non-zero only at specific points. Through detailed calculations, the topological number or total charge  $W$  can be expressed, involving the Hopf index and the sign of the topological current at zero points. The winding number, which is independent of the region's shape, directly relates to black hole stability. A positive winding number corresponds to a stable black hole state, while a negative winding number indicates instability. This topological approach provides a robust framework for understanding the stability and phase transitions of black holes, offering new insights into their thermodynamic behavior. The generalized free energy is determined as follows[20, 21]:

$$\mathcal{F} = M - \frac{S}{\tau}, \quad (21)$$

In this context,  $\tau$  represents the Euclidean time period, and its inverse,  $T$ , represents the system's temperature. The generalized free energy is considered on-shell only when  $\tau$  matches the inverse of the Hawking temperature. By applying CFT thermodynamics to examine the phase structure of black holes, we redefine the generalized Helmholtz energy within the CFT framework as follows:

$$\mathcal{F} = E - \frac{\tilde{S}}{\tilde{\tau}}. \quad (22)$$

In this context, the generalized Helmholtz energy is on-shell only when ( $\tilde{\tau} = \tilde{\tau}_H = \frac{1}{T_H}$ ). To facilitate this analysis, a vector ( $\phi$ ) is constructed with components derived from the partial derivatives as follows:

$$\phi = \left( \frac{\partial \mathcal{F}}{\partial r_H}, -\cot \Theta \csc \Theta \right). \quad (23)$$

In this scenario, ( $\phi^\Theta$ ) becomes infinite, and the vector points outward at the angles ( $\Theta = 0$ ) and ( $\Theta = \pi$ ). The permissible ranges for the horizon radius ( $r_H$ ) and the angle ( $\Theta$ ) are from 0 to infinity and from 0 to ( $\pi$ ), respectively. By applying Duan's ( $\phi$ )-mapping topological current theory, we can define a topological current as follows:

$$j^\mu = \frac{1}{2\pi} \varepsilon^{\mu\nu\rho} \varepsilon_{ab} \partial_\nu n^a \partial_\rho n^b, \quad \mu, \nu, \rho = 0, 1, 2, \quad (24)$$

In this formulation,  $n$  is defined as  $(n^1, n^2)$ , where  $(n^1 = \frac{\phi^r}{|\phi|})$  and  $(n^2 = \frac{\phi^s}{|\phi|})$ . According to the conservation equation, the current  $(j^\mu)$  is non-zero exclusively at the points where  $(\phi = 0)$ . After performing the necessary calculations, the topological number or total charge  $W$  can be determined as follows:

$$W = \int_{\Sigma} j^0 d^2x = \sum_{i=1}^n \beta_i \eta_i = \sum_{i=1}^n \omega_i. \quad (25)$$

In this context,  $(\beta_i)$  represents the positive Hopf index, which counts the number of loops made by the vector  $(\phi^a)$  in the  $(\phi)$ -space when  $(x^\mu)$  is close to the zero point  $(z_i)$ . Meanwhile,  $(\eta_i)$  is defined as the sign of  $(j^0(\phi/x)_{z_i})$ , which can be either +1 or -1. The term  $(\omega_i)$  denotes the winding number associated with the  $i$ -th zero point of  $(\phi)$  within the region  $(\Sigma)$ .

#### IV. NON-EXTENSIVE ENTROPY

Non-extensive entropy, proposed by Tsallis, is an extension of the traditional Boltzmann-Gibbs entropy. This concept is particularly valuable for systems with non-linear dynamics and strong initial condition dependencies. Unlike Boltzmann-Gibbs entropy, which assumes linear scaling with system size, non-extensive entropy can manage systems where this linearity is absent. This makes it relevant to various fields, including theoretical physics, cosmology, and statistical mechanics, especially for systems with long-range interactions, fractal structures, or memory effects[74–76].

- Rényi entropy is a type of non-extensive entropy applied in black hole thermodynamics. It is characterized by a parameter that adjusts the degree of non-extensiveness, which must be within a specific range to ensure the entropy function is well-defined. When used for black holes, Rényi entropy offers a framework for understanding their thermodynamic properties, extending traditional Boltzmann-Gibbs statistics[77–79].

$$S_R = \frac{1}{\lambda} \ln(1 + \lambda S_{BH}) \quad (26)$$

The parameter  $(\lambda)$  in non-extensive entropy is essential for defining the entropy function. For the entropy function to be well-defined,  $(\lambda)$  must be within the range  $(-\infty < \lambda < 1)$ . Values outside this range make the entropy function convex and thus ill-defined. In black hole thermodynamics using Rényi statistics, the entropy  $(S_R)$  is properly defined when  $(\lambda)$  is between 0 and 1. Within this range,  $(\lambda)$  shows favorable thermodynamic properties, as recent studies have demonstrated. Notably, as the Rényi parameter  $(\lambda)$  approaches zero, the generalized off-shell free energy converges to classical Boltzmann-Gibbs statistics.

- Sharma-Mittal entropy is another significant form of non-extensive entropy, generalizing both Rényi and Tsallis entropies. This entropy has been particularly useful in cosmological studies, such as explaining the accelerated expansion of the universe by effectively utilizing vacuum energy. Although non-extensive entropies have been used to study black holes, Sharma-Mittal entropy has not been extensively applied in this context. This presents an opportunity to explore the thermodynamic properties of black holes using Sharma-Mittal entropy, considering them as strongly coupled gravitational systems[81–83].

$$S_{SM} = \frac{1}{\alpha} \left( (1 + \beta S_T)^{\frac{\alpha}{\beta}} - 1 \right). \quad (27)$$

In this context,  $S_T$  represents the Tsallis entropy, derived from the horizon area  $(A = 4\pi r^2)$ , where  $r$  is the radius of the black hole's event horizon. The parameters  $\alpha$  and  $(\beta)$  are adjustable and need to be calibrated using observational data. Interestingly, when  $\alpha$  approaches zero, Sharma-Mittal entropy simplifies to Rényi entropy. Similarly, when  $\alpha$  equals  $(\beta)$ , it reduces to Tsallis entropy.

- Non-extensive statistical mechanics in Loop Quantum Gravity provides the entropy[84–86]

$$S_q = \frac{1}{1-q} \left[ e^{(1-q)\Lambda(\gamma_0)S} - 1 \right], \quad (28)$$

where the entropic index  $q$  quantifies how the probability of frequent events is enhanced relative to infrequent ones,

$$\Lambda(\gamma_0) = \frac{\ln 2}{\sqrt{3}\pi\gamma_0}, \quad (29)$$

and  $\gamma_0$  is the Barbero-Immirzi parameter, typically assumed to take one of the two values  $\frac{\ln 2}{\pi\sqrt{3}}$  or  $\frac{\ln 3}{2\pi\sqrt{2}}$ , depending on the gauge group used in Loop Quantum Gravity. However,  $\gamma_0$  is a free parameter in scale-invariant gravity[87–90]. With the first choice of  $\gamma_0$ ,  $\Lambda(\gamma_0)$  becomes unity, and the entropy reduces to the Bekenstein-Hawking form in the limit  $q \rightarrow 1$ , corresponding to extensive statistical mechanics. This Loop Quantum Gravity entropy has been applied to black holes in[84, 85] and to cosmology in[86].

## V. THERMODYNAMIC TOPOLOGY AND THE RÉNYI ENTROPY

The application of Rényi entropy in black hole models can yield interesting consequences and provide new insights into the complex structure of general relativity. Based Eqs. 14, 22 and 26, the generalized Helmholtz free energy we have:

$$\mathcal{F} = \frac{(768x^6C^2\pi^2 + 768x^4C^2\pi^2 + 768yx^2C^2\pi^2 + Q^2k^2)\Sigma}{256x^2(\mathcal{V}k^2)^{\frac{1}{3}}C\pi^2} - \frac{\ln\left(1 + \frac{4(x^3+6yx)\Sigma C\pi\lambda}{k}\right)}{\lambda\tilde{\tau}} \quad (30)$$

With respect to Bekenstein-Hawking entropy,

$$S_{BH} = \frac{4(x^3 + 6yx)\Sigma C\pi}{k}. \quad (31)$$

Also, the Rényi entropy will be,

$$S_R = \frac{\ln\left(1 + \frac{4(x^3+6yx)\Sigma C\pi\lambda}{k}\right)}{\lambda}. \quad (32)$$

Now form Eq.23 for components of the vector field  $\Phi$  and  $\tilde{\tau}$  we have:

$$\begin{aligned} \varphi_1 &= x^3C^2\left(-4x^2\tilde{\tau}\left(x^2 + \frac{1}{2}\right)\lambda(x^2 + 6y)\Sigma C + (x^2 + 2y)(\mathcal{V}k^2)^{\frac{1}{3}}\right)\pi^3 - x^4kC^2\left(x^2 + \frac{1}{2}\right)\tilde{\tau}\pi^2, \\ \phi^x &= -\frac{3\left(\varphi_1 + \frac{CQ^2\Sigma k^2\lambda\tilde{\tau}x(x^2+6y)\pi}{384} + \frac{Q^2k^3\tilde{\tau}}{1536}\right)\Sigma}{(\mathcal{V}k^2)^{\frac{1}{3}}\left(C\lambda x\Sigma(x^2 + 6y)\pi + \frac{k}{4}\right)x^3\tilde{\tau}C\pi^2}, \end{aligned} \quad (33)$$

$$\phi^\theta = -\frac{\cos(\theta)}{\sin(\theta)^2} \quad (34)$$

$$\tilde{\tau}_1 = 6144C^3\pi^3\Sigma\lambda x^9 + 36864C^3\pi^3\Sigma\lambda x^7y + 3072C^3\pi^3\Sigma\lambda x^7 + 18432C^3\pi^3\Sigma\lambda x^5y + 1536C^2\pi^2kx^6$$

$$\tilde{\tau} = \frac{1536(x^2 + 2y)C^2\pi^3x^3(\mathcal{V}k^2)^{\frac{1}{3}}}{-4C\pi Q^2\Sigma k^2\lambda x^3 - 24C\pi Q^2\Sigma k^2\lambda xy + 768C^2\pi^2kx^4 - Q^2k^3 + \tilde{\tau}_1} \quad (35)$$

In order to better observe the effect of the Rényi entropy and it's parameter changes on phase transition, we divide our studies into two parts. In the first case, we will examine the phase behavior of the sample below critical  $C$ , and in the second case, we will go to values greater than critical  $C$ .

### A. $C = 0.15 < C_c$

First, it is better to examine the effect of changing  $\lambda$  on  $\tilde{\tau}$  (the temperature inverse).

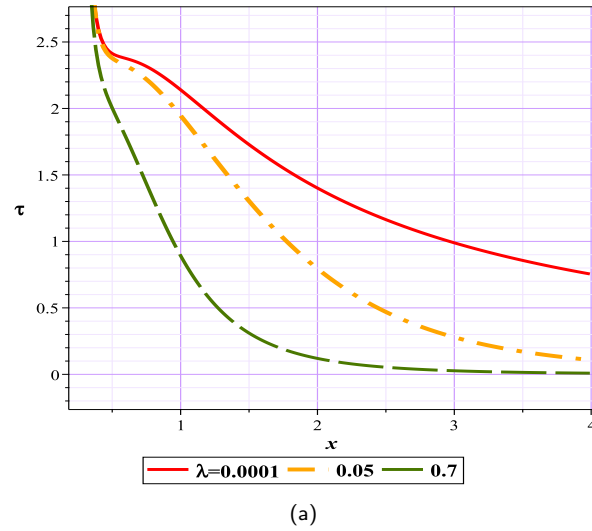


FIG. 1. ( $\bar{\tau}$  VS  $x$ ) with different  $\lambda$  for 5D G-B black hole model and Rényi entropy

As can be seen in Fig. 1, in this case, changes in  $\lambda$  do not seem to cause the  $\tau$  function to have an extremum. Therefore, we expect that for any choice of value for this function, a topological charge of  $+1$  will always appear, which can be clearly seen in Fig. 2. In fact, below the critical  $C$ , the sample will seem to experience only one second-order phase transition.

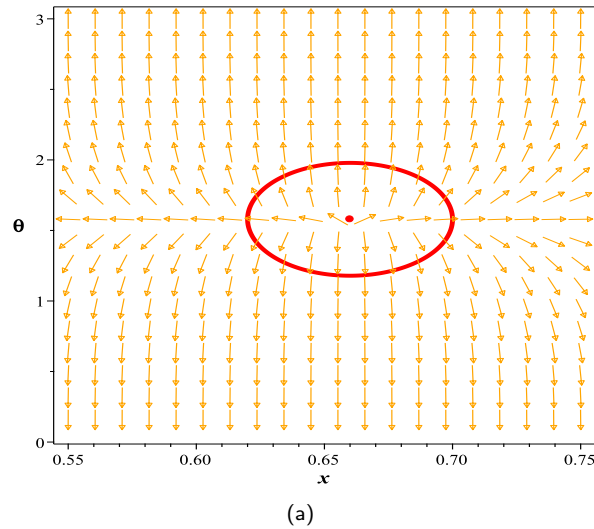


FIG. 2. The normal vector field  $n$  in the  $(x - \theta)$  plane. The ZP(Zero Points) is located at  $(x, \theta) = (0.66, 1.57)$  with respect to  $(\lambda = 0.0001, \nu = 1, k = 1, Q = 1, \Sigma = 1, C = 0.15, y = 0.01)$

### B. $C = 2.5 > C_c$

At values greater than the critical  $C$ , the black hole's phase behavior appears to be completely different.



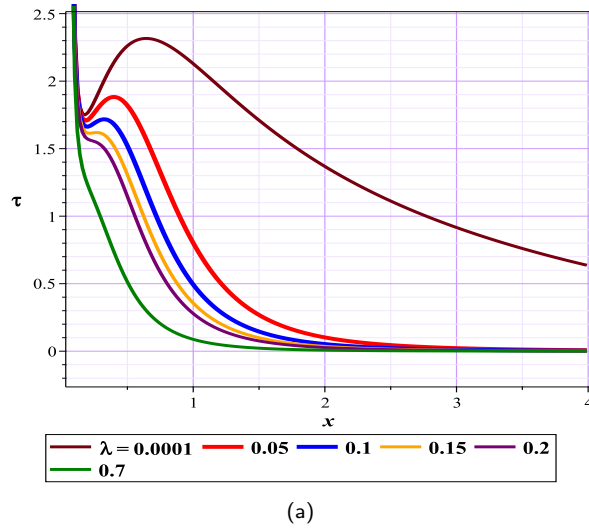


FIG. 3. ( $\tau$  VS  $x$ ) with different  $\lambda$  for 5D G-B black hole model and Rényi entropy

As can be seen in Fig. 3, the phase behavior of the black hole will be affected by the choice of the  $\lambda$  parameter and clearly, depending on our choice, each can experience both forms of phase transition. At very small  $\lambda$  (burgundy line), the intensity of the changes is very high. We know that this very small  $\lambda$  means moving towards the Bekenstein-Hawking entropy. In other words, it can be said with certainty that the structure in the usual Bekenstein-Hawking entropy and below the critical  $C$  will definitely experience a first-order phase transition. But in the case of our study, for example for  $\lambda = 0.05$  (red line), we can clearly see that extrema in the  $\tilde{\tau}$  function have appeared. This means that a ZP with topological charge -1 (green contour) will definitely appear in the topological study, Fig. 4. This means that our black hole will pass through an unstable intermediate black hole (which appears and then disappears) during the phase transition from a small to a large black hole, and will experience a creation point and an annihilation point in this transition.

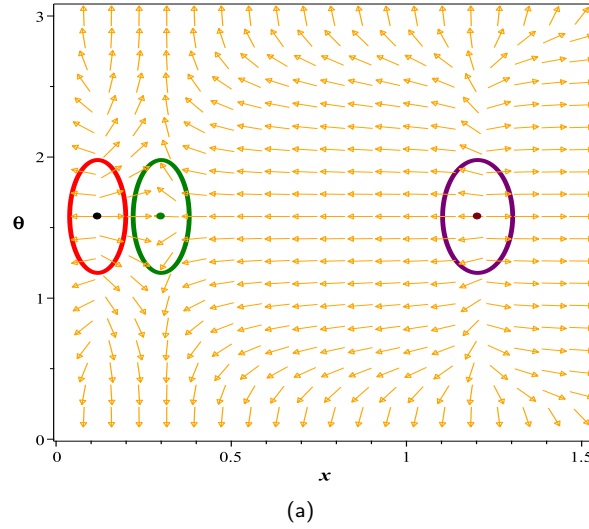


FIG. 4. The normal vector field  $n$  in the  $(x - \theta)$  plane. The ZPs are located at  $(x, \theta) = (0.1187834875, 1.57)$ ,  $(x, \theta) = (0.2999999998, 1.57)$ ,  $(x, \theta) = (1.203156012, 1.57)$  with respect to  $(\lambda = 0.0001, \mathcal{V} = 1, k = 1, Q = 1, \Sigma = 1, C = 2.5, y = 0.01, \tilde{\tau} = 1.956446998)$

As can be seen in Fig. 3, around  $\lambda = 0.15$ , the extrema of the  $\tilde{\tau}$  function disappear and the intermediate black hole is effectively eliminated. This means that the phase transition takes on a second-order form and a continuous gradual transformation will transform the small black hole into a large black hole. This trend is also true for values larger than 0.15.

## VI. THERMODYNAMIC TOPOLOGY AND SHARMA-MITTAL ENTROPY

Using equations (14), (15), and (22), we can rewrite the generalized Helmholtz energy for the Sharma-Mittal entropy as follows,

$$\mathcal{F} = \frac{\Sigma \left( 768C^2 (x^4 + x^2 + y) + \frac{k^2 Q^2}{\pi^2 x^2} \right)}{256Ck^{2/3} \sqrt[3]{\mathcal{V}}} - \frac{\left( \frac{4\pi\beta C \Sigma (x^3 + 6xy)}{k} + 1 \right)^{\alpha/\beta} - 1}{\alpha \tilde{\tau}} \quad (36)$$

From (23), for the components of the vector field  $\Phi$  and  $\tilde{\tau}$ , we obtain:

$$\phi^x = \frac{6C\Sigma}{\ell} \left( \frac{2x^3 + x}{k^{2/3} \sqrt[3]{\mathcal{V}}} - \frac{2\pi (x^2 + 2y) \left( \frac{4\pi\beta C \Sigma x (x^2 + 6y)}{k} + 1 \right)^{\frac{\alpha}{\beta} - 1}}{k \tilde{\tau}} \right) \quad (37)$$

$$\phi^\theta = -\frac{\cot(\theta)}{\sin(\theta)} \quad (38)$$

$$\tilde{\tau} = \frac{1536\pi^3 C^2 \sqrt[3]{\mathcal{V}} x^3 (x^2 + 2y) \left( \frac{4\pi\beta C \Sigma x (x^2 + 6y)}{k} + 1 \right)^{\frac{\alpha}{\beta} - 1}}{\sqrt[3]{k} (768\pi^2 C^2 x^4 (2x^2 + 1) - k^2 Q^2)} \quad (39)$$

### A. $C = 0.15 < C_c$

In this scenario, where no first-order phase transition takes place, two distinct topological charges can exist: for  $\alpha > \beta$  (Fig. (5)), the total topological charge is +1, while for  $\alpha \leq \beta$  (Fig. (6)), it is 0. Next, we will analyze the scenario in

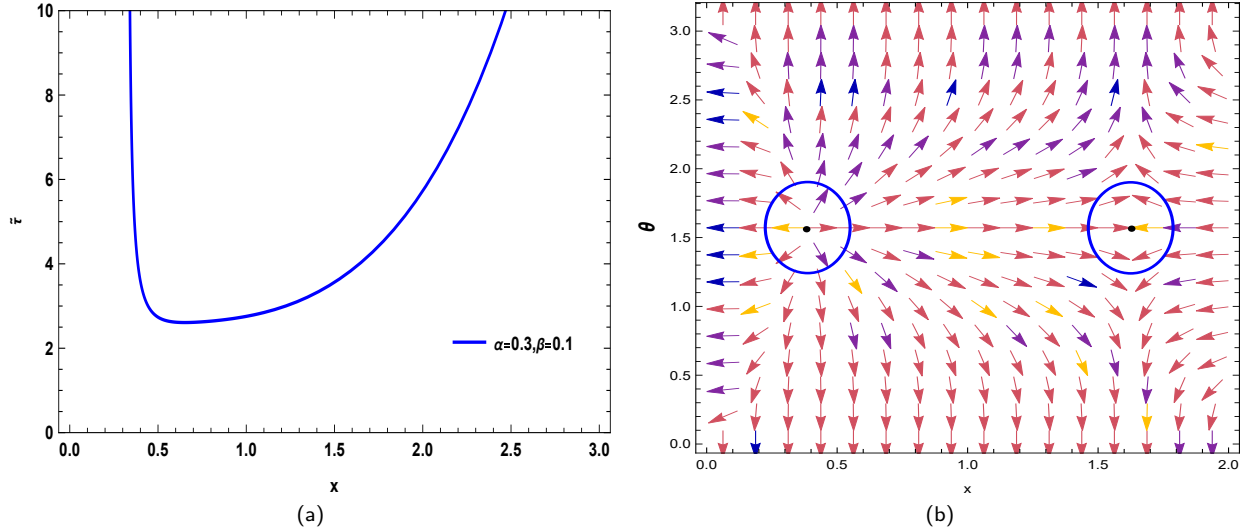


FIG. 5. (a) The plot of the curve of equation (39) with respect to  $k = \mathcal{V} = Q = \ell = \Sigma = 1$ ,  $y = 0.01$ ,  $\alpha = 0.3$ ,  $\beta = 0.1$  and  $C = 0.1 < C_c = 0.187$  (b), the blue arrows represent the vector field  $n$  on a portion of the  $(x - \theta)$  plane for the quantum-corrected (AdS-RN) black holes in Kiselev spacetime. The blue loops enclose the ZPs  $\tilde{\tau} = 4$ .

which a first-order phase transition takes place.

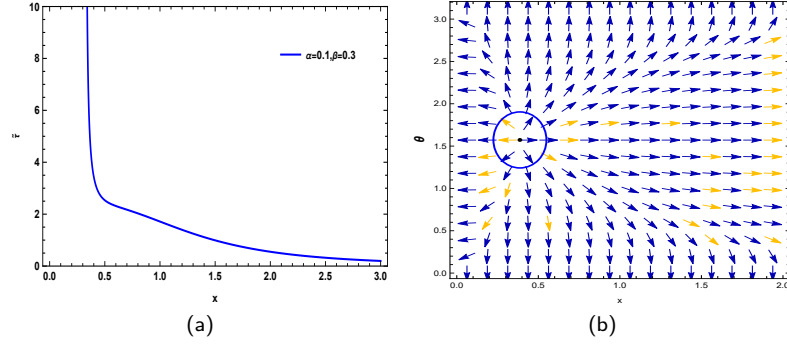


FIG. 6. (a) The plot of the curve of equation (17) with respect to  $k = \mathcal{V} = Q = \ell = \Sigma = 1$ ,  $y = 0.01$ ,  $\alpha = 0.1, \beta = 0.3$  and  $C = 0.1 < C_c = 0.187$  (b), the blue arrows represent the vector field  $n$  on a portion of the  $(x - \theta)$  plane for the Einstein-Gauss-Bonnet black holes. The blue loops enclose the ZPs  $\tilde{\tau} = 4$ .

### B. $C = 2.5 > C_c$

In this scenario, a first-order phase transition occurs for the black hole when considering the Bekenstein-Hawking entropy. However, the situation shifts when the Sharma-Mittal entropy is applied. When  $\alpha > \beta$  (Fig. (9)), the total topological charge is 0. When  $\alpha$  and  $\beta$  are close together ( $\alpha \approx \beta$ ), the topological charge is +1 (Figs. (7),(8)). Similarly, when  $\alpha < \beta$ , the topological charge is also +1 (Fig. (10)).

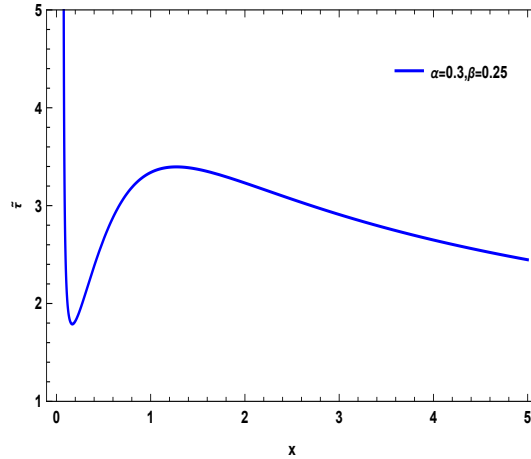


FIG. 7. The plot of the curve of equation (39) with respect to  $k = \mathcal{V} = Q = \ell = \Sigma = 1$ ,  $y = 0.01$ ,  $\alpha = 0.3, \beta = 0.25$  and  $C > C_c = 2.5$

## VII. THERMODYNAMIC TOPOLOGY WITHIN LQG

In this study, we investigate the thermodynamic topology of Einstein-Gauss-Bonnet black holes within the context of LQG and the CFT. By utilizing Eqs. (28), (21), we derive the function  $\mathcal{F}$ .

$$\mathcal{F} = \frac{\Sigma (768\pi^2 c^2 x^6 + 768\pi^2 c^2 x^4 + 768\pi^2 c^2 x^2 y + k^2 Q^2)}{256\pi^2 c k^{2/3} \sqrt[3]{\mathcal{V}} x^2} - \frac{e^{\frac{4\pi c(1-q)\Sigma(x^3+6xy)}{k}} - 1}{(1-q)\tilde{\tau}} \quad (40)$$

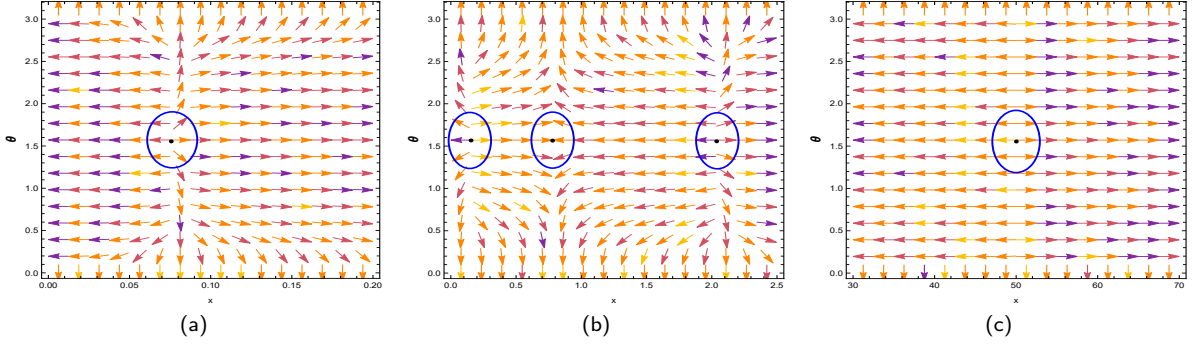


FIG. 8. the blue arrows represent the vector field  $n$  on a portion of the  $(x - \theta)$  plane for Einstein-Gauss-Bonnet black holes. The blue loops enclose the ZPs with respect to  $k = \mathcal{V} = Q = \ell = \Sigma = 1$ ,  $y = 0.01$ ,  $\alpha = 0.3$ ,  $\beta = 0.25$  and  $C = 2.5 > C_c = 0.187$  (a)  $\tilde{\tau} = 4$  (b)  $\tilde{\tau} = 3.2$ , (c)  $\tilde{\tau} = 1$

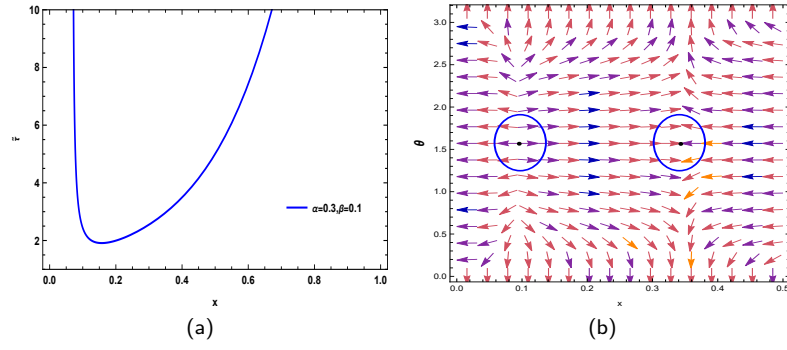


FIG. 9. (a) The plot of the curve of equation(39) with respect to  $k = \mathcal{V} = Q = \ell = \Sigma = 1$ ,  $y = 0.01$ ,  $\alpha = 0.3$ ,  $\beta = 0.1$  and  $C = 2.5 > C_c = 0.187$  (b), the blue arrows represent the vector field  $n$  on a portion of the  $(x - \theta)$  plane for Einstein-Gauss-Bonnet black holes. The blue loops enclose the ZPs  $\tilde{\tau} = 3$ .

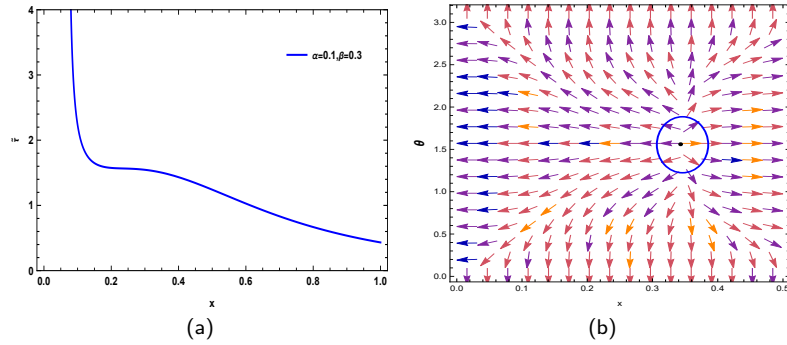


FIG. 10. (a) The plot of the curve of equation (39) with respect to  $k = \mathcal{V} = Q = \ell = \Sigma = 1$ ,  $y = 0.01$ ,  $\alpha = 0.1$ ,  $\beta = 0.3$  and  $C = 2.5 > C_c = 0.187$  (b), the blue arrows represent the vector field  $n$  on a portion of the  $(x - \theta)$  plane for Einstein-Gauss-Bonnet black holes. The blue loops enclose the ZPs  $\tilde{\tau} = 1.5$ .

Then, by using Eqs. (23), the  $\phi^{r_h}$  and  $\phi^\theta$  are obtained as follows,

$$\phi^x = \frac{\Sigma (4608\pi^2 c^2 x^5 + 3072\pi^2 c^2 x^3 + 1536\pi^2 c^2 xy)}{256\pi^2 c k^2 / 3 \sqrt[3]{\mathcal{V} x^2}} - \frac{\Sigma (768\pi^2 c^2 x^6 + 768\pi^2 c^2 x^4 + 768\pi^2 c^2 x^2 y + k^2 Q^2)}{128\pi^2 c k^2 / 3 \sqrt[3]{\mathcal{V} x^3}} - \frac{4\pi c \Sigma (3x^2 + 6y) e^{\frac{4\pi c(1-q)\Sigma(x^3+6xy)}{k}}}{k\tilde{\tau}} \quad (41)$$

and

$$\phi^\theta = -\frac{\cot(\theta)}{\sin(\theta)} \quad (42)$$

We can calculate the  $\tau$  as follows,

$$\tilde{\tau} = \frac{1536\pi^3 \left( 2c^2 \sqrt[3]{v} x^3 y e^{\frac{4\pi c(1-q)\Sigma(x^3+6xy)}{k}} + c^2 \sqrt[3]{v} x^5 e^{\frac{4\pi c(1-q)\Sigma(x^3+6xy)}{k}} \right)}{1536\pi^2 c^2 \sqrt[3]{k} x^6 + 768\pi^2 c^2 \sqrt[3]{k} x^4 - k^{7/3} Q^2} \quad (43)$$

Here, we delve into the thermodynamic topology of Einstein-Gauss-Bonnet black holes within the framework of the CFT, taking into account the effects of non-extensive entropy formulations such as LQG. The illustrations are divided, with normalized field lines shown on the right. Figs.(11) and (12) illustrate the results for  $C < C_c$  and  $C > C_c$ , respectively. Figs. (11(b)), (11(d)), and (11(f)) depict two zero points for  $C < C_c$ , while Figs. (12(b)), (12(d)), and (12(f)) show two zero points for  $C > C_c$ . These zero points, representing topological charges, are determined by the free and non-extensive parameters  $q$  and are located within the blue contour loops at coordinates  $(r, \theta)$ . The sequence of these illustrations is governed by the parameter  $q$ . The findings from these figures reveal a distinctive feature: two topological charges ( $\omega = +1, -1$ ) and the total topological charge  $W = 0$ , indicated by the zero points within the contour. Our analysis evaluates black hole stability by examining the winding numbers. Additionally, as shown in Fig. (11(h)) for  $C < C_c$  and Fig. (12(h)) for  $C > C_c$ , when the parameter  $q$  increases to 1, the classification changes. We observe one and three topological charges with a total topological charge  $W = +1$ . Fig. (11(h)) shows one topological charge ( $\omega = +1$ ) with the total topological charge  $W = +1$ , while Fig. (12(h)) shows three topological charges ( $\omega = +1, -1, +1$ ) with the total topological charge  $W = +1$ .

#### A. Case I: $C = 0.15 < C_c$

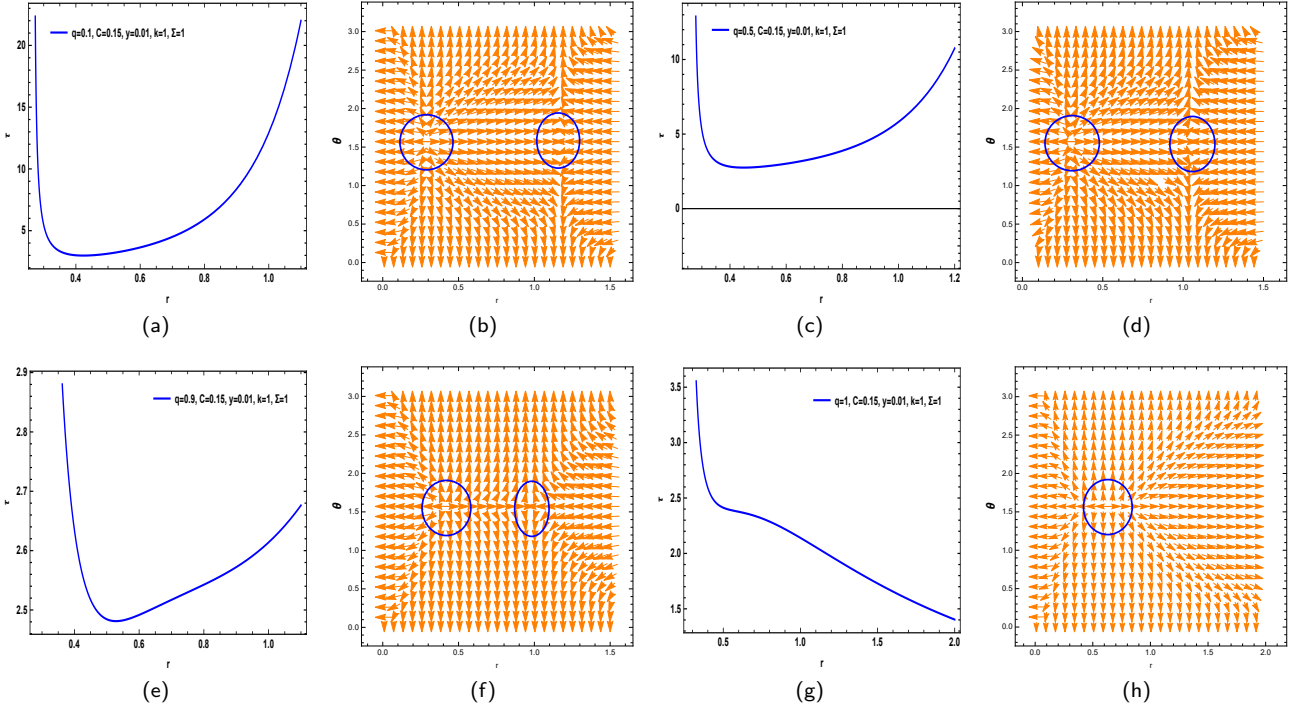


FIG. 11. The curve defined by Eq. (43) is depicted in Figs. (11(a)), (11(c)), (11(e)), and (11(g)). In Figs. (11(b)), (11(d)), (11(f)), and (11(h)), the zero points (ZPs) are positioned at coordinates  $(r, \theta)$  which correspond to the free parameters,  $r=x$  with  $\ell = 1$ .

### B. Case II: $C = 2.5 > C_c$

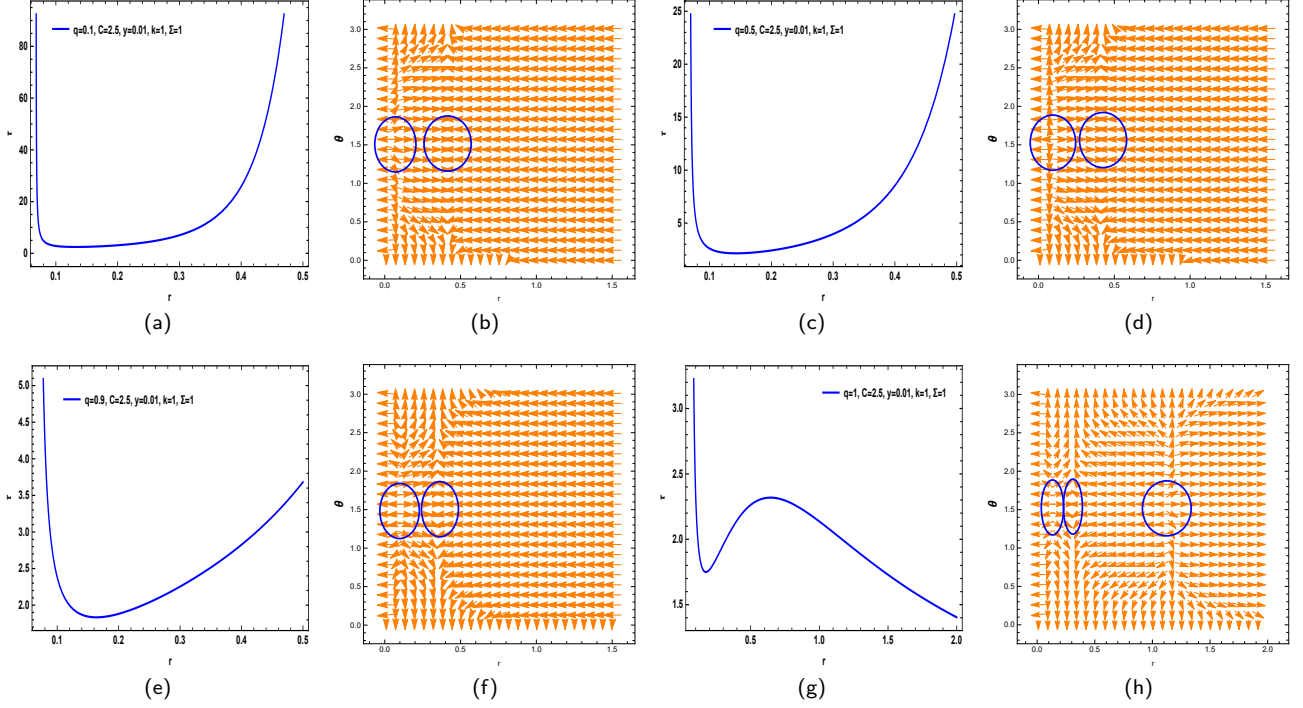


FIG. 12. The curve represented by Eq. (43) is shown in Figs. (12(a)), (12(c)), (12(e)), and (12(g)). In Figs. (12(b)), (12(d)), (12(f)), and (12(h)), the zero points (ZPs) are identified at coordinates  $(r, \theta)$  which correspond to the free parameters,  $r=x$  with  $\ell = 1$

## VIII. CONCLUSIONS

We conducted an in-depth investigation into the thermodynamic topology of Einstein-Gauss-Bonnet black holes within the framework of Conformal Field Theory (CFT), considering the implications of non-extensive entropy formulations. The intriguing results obtained in this study are as follows:

The choice of the parameter  $\lambda$  below the critical value ( $C$ ) has practically no effect on the phase behavior of the black hole. However, when  $\lambda$  exceeds the critical value ( $C$ ), this choice can significantly alter the phase transition outcome of the black hole. Determining which values of  $\lambda$  best represent physical reality will undoubtedly require experimental evidence. Nevertheless, this flexibility in choosing the parameter can provide researchers with greater freedom to explain the events occurring during a black hole phase transition, depending on the physical conditions.

When the Sharma-Mittal entropy is incorporated into the Helmholtz free energy to study phase transitions, the parameters  $\alpha$  and  $\beta$  can influence both the phase transition and the topological charge. Specifically, if  $\alpha > \beta$ , the topological charge is 0, whereas for  $\alpha \leq \beta$ , the topological charge is +1. Also, for LQG, As the parameter  $q$  increases to 1, the classification changes. We observe one and three topological charges with the total topological charge ( $W = +1$ ) with respect to  $C_c$ . In other cases, we encounter two topological charges ( $\omega = +1, -1$ ), leading to a total topological charge ( $W = 0$ ).

- 
- [1] Maldacena J. The large- $N$  limit of superconformal field theories and supergravity. International journal of theoretical physics. 1999 Apr;38(4):1113-33.  
 [2] Ramallo AV. Introduction to the AdS/CFT correspondence. In Lectures on Particle Physics, Astrophysics and Cosmology: Proceedings of the Third IDPASC School, Santiago de Compostela, Spain, January 21–February 2, 2013 2015 (pp. 411-474). Springer International Publishing.

- [3] Di Vecchia P. An introduction to AdS/CFT correspondence. *Fortschritte der Physik: Progress of Physics*. 2000 Jan;48(1-3):87-92.
- [4] Witten E. Anti-de Sitter space, thermal phase transition, and confinement in gauge theories. arXiv preprint [hep-th/9803131](https://arxiv.org/abs/hep-th/9803131). 1998 Mar 16.
- [5] Compere G, Marolf D. Setting the boundary free in AdS/CFT. *Classical and quantum gravity*. 2008 Sep 16;25(19):195014. Genolini PB, Richmond P, Sparks J. Gravitational free energy in topological AdS/CFT. *Journal of High Energy Physics*. 2018 Sep;2018(9):1-40.
- [6] Sadeghi J, Alipour MR, Afshar MA, Noori Gashti S. Exploring the phase transition in charged Gauss–Bonnet black holes: a holographic thermodynamics perspectives. *General Relativity and Gravitation*. 2024 Aug;56(8):93.
- [7] Sadeghi J, Afshar MA, Gashti SN, Alipour MR. Kramer’s Escape Rate and Phase Transition Dynamics in AdS Black Holes with Dark Structures. arXiv preprint [arXiv:2404.17849](https://arxiv.org/abs/2404.17849). 2024 Apr 27.
- [8] Sadeghi J, Afshar MA, Alipour MR, Gashti SN. Phase transition dynamics of black holes influenced by Kaniadakis and Barrow statistics. *Physics of the Dark Universe*. 2024 Dec 17:101780.
- [9] Cunha, Pedro VP, and Carlos AR Herdeiro. "Stationary black holes and light rings." *Physical Review Letters* 124.18 (2020): 181101.
- [10] Cunha, Pedro VP, Emanuele Berti, and Carlos AR Herdeiro. "Light-ring stability for ultracompact objects." *Physical review letters* 119.25 (2017): 251102.
- [11] Wei, Shao-Wen. "Topological charge and black hole photon spheres." *Physical Review D* 102.6 (2020): 064039.
- [12] Sadeghi J, Afshar MA. The role of topological photon spheres in constraining the parameters of black holes. *Astroparticle Physics*. 2024 Jun 9:10299.
- [13] Afshar MA, Sadeghi J. Effective potential and topological photon spheres: a novel approach to black hole parameter classification. arXiv preprint [arXiv:2405.18798](https://arxiv.org/abs/2405.18798). 2024 May 29.
- [14] Afshar MA, Sadeghi J. Black Hole Orbit Classification: The Synergistic Effects of Cloud Strings, Gauss-Bonnet Terms, and Non-Commutative Parameters in Identifying WGC candidate Models: WGC as WCCC protector. arXiv preprint [arXiv:2412.00079](https://arxiv.org/abs/2412.00079). 2024 Nov.
- [15] Afshar MA, Sadeghi J. Mutual Influence of Photon Sphere and Non-Commutative Parameter in Various Non-Commutative Black Holes: Part I-Towards evidence for WGC. arXiv preprint [arXiv:2411.09557](https://arxiv.org/abs/2411.09557). 2024 Nov 14
- [16] Afshar MA, Sadeghi J. Mechanisms Behind the Aschenbach Effect in Non-Rotating Black Hole Spacetime. arXiv preprint [arXiv:2412.06357](https://arxiv.org/abs/2412.06357). 2024 Dec 9.
- [17] Alipour MR, Afshar MA, Gashti SN, Sadeghi J. Weak Gravity Conjecture Validation with Photon Spheres of Quantum Corrected AdS-Reissner-Nordstrom Black Holes in Kiselev Spacetime. arXiv preprint [arXiv:2410.14352](https://arxiv.org/abs/2410.14352). 2024 Oct 18.
- [18] Liu W, Wu D, Wang J. Light rings and shadows of static black holes in effective quantum gravity II: A new solution without Cauchy horizons. arXiv preprint [arXiv:2412.18083](https://arxiv.org/abs/2412.18083). 2024 Dec 24.
- [19] Liu W, Wu D, Wang J. Light rings and shadows of static black holes in effective quantum gravity. *Physics Letters B*. 2024 Nov 1;858:139052.
- [20] Wei, Shao-Wen, and Yu-Xiao Liu. "Topology of black hole thermodynamics." *Physical Review D* 105.10 (2022): 104003.
- [21] Wei, Shao-Wen, Yu-Xiao Liu, and Robert B. Mann. "Black hole solutions as topological thermodynamic defects." *Physical Review Letters* 129.19 (2022): 191101.
- [22] Bai, Ning-Chen, Lei Li, and Jun Tao. "Topology of black hole thermodynamics in Lovelock gravity." *Physical Review D* 107.6 (2023): 064015.
- [23] Yerra, Pavan Kumar, and Chandrasekhar Bhamidipati. "Topology of Born-Infeld AdS black holes in 4D novel Einstein-Gauss-Bonnet gravity." *Physics Letters B* 835 (2022): 137591.
- [24] D Wu, Wu SQ. Topological classes of thermodynamics of rotating AdS black holes. *Physical Review D*. 2023 Apr 15;107(8):084002.
- [25] D Wu, Gu SY, Zhu XD, Jiang QQ, Yang SZ. Topological classes of thermodynamics of the static multi-charge AdS black holes in gauged supergravities: novel temperature dependent thermodynamic topological phase transition. *Journal of High Energy Physics*. 2024 Jun;2024(6):1-35.
- [26] Zhu XD, Liu W, D Wu. Universal thermodynamic topological classes of rotating black holes. *Physics Letters B*. 2024 Nov 29:139163.
- [27] Zhu XD, D Wu, Wen D. Topological classes of thermodynamics of the rotating charged AdS black holes in gauged supergravities. arXiv preprint [arXiv:2402.15531](https://arxiv.org/abs/2402.15531). 2024 Feb 22.
- [28] Liu W, Zhang L, D Wu, Wang J. Thermodynamic topological classes of the rotating, accelerating black holes. arXiv preprint [arXiv:2409.11666](https://arxiv.org/abs/2409.11666). 2024 Sep 18.
- [29] D Wu, Liu W, Wu SQ, Mann RB. Novel Topological Classes in Black Hole Thermodynamics. arXiv preprint [arXiv:2411.10102](https://arxiv.org/abs/2411.10102). 2024 Nov 15
- [30] D Wu, "Classifying topology of consistent thermodynamics of the four-dimensional neutral Lorentzian NUT-charged spacetimes." *The European Physical Journal C* 83.5 (2023):365.
- [31] D Wu, "Consistent thermodynamics and topological classes for the four-dimensional Lorentzian charged Taub-NUT spacetimes." *The European Physical Journal C* 83.7 (2023):589.
- [32] Chen H, D Wu, Zhang MY, Hassanabadi H, Long ZW. Thermodynamic topology of phantom AdS black holes in massive gravity. *Physics of the Dark Universe*. 2024 Dec 1;46:101617
- [33] Sadeghi J, Gashti SN, Alipour MR, Afshar MA. Bardeen black hole thermodynamics from topological perspective. *Annals of Physics*. 2023 Aug 1;455:169391.
- [34] Sadeghi J, Afshar MA, Gashti SN, Alipour MR. Thermodynamic topology of black holes from bulk-boundary, extended, and restricted phase space perspectives. *Annals of Physics*. 2024 Jan 1;460:169569.

- [35] Alipour MR, Afshar MA, Gashti SN, Sadeghi J. Topological classification and black hole thermodynamics. *Physics of the Dark Universe*. 2023 Dec 1;42:101361.
- [36] Sadeghi J, Alipour MR, Gashti SN, Afshar MA. Bulk-boundary and RPS Thermodynamics from Topology perspective. *Chinese Physics C* 48, 095106. 2024 Jun 28.
- [37] Sadeghi J, Gashti SN, Alipour MR, Afshar MA. Thermodynamic topology of quantum corrected AdS-Reissner-Nordstrom black holes in Kiselev spacetime. *Chinese Physics C*. 2024 Nov 1;48(11):115115.
- [38] Sadeghi J, Afshar MA, Gashti SN, Alipour MR. Topology of Hayward-AdS black hole thermodynamics. *Physica Scripta*. 2024 Jan 4;99(2):025003.
- [39] Sadeghi J, Afshar MA, Gashti SN, Alipour MR. Thermodynamic topology and photon spheres in the hyperscaling violating black holes. *Astroparticle Physics*. 2024 Apr 1;156:102920.
- [40] Sekhmani Y, Gashti SN, Afshar MA, Alipour MR, Sadeghi J, Rayimbaev J. Thermodynamic topology of Black Holes in  $F(R)$ -Euler-Heisenberg gravity's Rainbow. arXiv preprint [arXiv:2409.04997](https://arxiv.org/abs/2409.04997). 2024 Sep 8.
- [41] Gashti SN, Afshar MA, Alipour MR, Sekhmani Y, Sadeghi J, Rayimbaeva J. Thermodynamic Topology of Kiselev-AdS Black Holes within  $f(R, T)$  gravity. arXiv preprint [arXiv:2410.02262](https://arxiv.org/abs/2410.02262). 2024 Oct 3.
- [42] Gashti SN, Pourhassan B. Non-extensive Entropy and Holographic Thermodynamics: Topological Insights. arXiv preprint [arXiv:2412.12132](https://arxiv.org/abs/2412.12132). 2024 Dec 6.
- [43] Gashti SN, Pourhassan B, Sakalli I. Thermodynamic Topology and Phase Space Analysis of AdS Black Holes Through Non-Extensive Entropy Perspectives. arXiv preprint [arXiv:2412.12137](https://arxiv.org/abs/2412.12137). 2024 Dec 7.
- [44] Gashti SN. Topology of Holographic Thermodynamics within Non-extensive Entropy. arXiv preprint [arXiv:2412.00889](https://arxiv.org/abs/2412.00889). 2024 Dec 1.
- [45] Gogoi NJ, Phukon P. Thermodynamic topology of 4D dyonic AdS black holes in different ensembles. *Physical Review D*. 2023 Sep 15;108(6):066016.
- [46] Hazarika B, Phukon P. Thermodynamic topology of black holes in  $f(R)$  gravity. *Progress of Theoretical and Experimental Physics*. 2024 Apr;2024(4):043E01.
- [47] Panah BE, Hazarika B, Phukon P. Thermodynamic topology of topological black hole in  $F(R)$ -ModMax gravity's rainbow. arXiv preprint [arXiv:2405.20022](https://arxiv.org/abs/2405.20022). 2024 May 30.
- [48] Hazarika B, Awal MB, Phukon P. The Interconnection of Cosmological Constant and Rényi Entropy in Kalb-Ramond Black Holes: Insights from Thermodynamic Topology. arXiv preprint [arXiv:2412.09494](https://arxiv.org/abs/2412.09494). 2024 Dec 12.
- [49] Hazarika B, Panah BE, Phukon P. Thermodynamic topology of topological charged dilatonic black holes. *The European Physical Journal C*. 2024 Nov;84(11):1-8.
- [50] Zhang MY, Zhou HY, Chen H, Hassanabadi H, Long ZW. Topological classification of critical points for hairy black holes in Lovelock gravity. *The European Physical Journal C*. 2024 Dec;84(12):1-0.
- [51] Chen H, Wu D, Zhang MY, Hassanabadi H, Long ZW. Thermodynamic topology of phantom AdS black holes in massive gravity. *Physics of the Dark Universe*. 2024 Dec 1;46:101617.
- [52] Zhang MY, Chen H, Hassanabadi H, Long ZW, Yang H. Thermodynamic topology of Kerr-Sen black holes via Rényi statistics. *Physics Letters B*. 2024 Sep 1;856:138885.
- [53] Zhang MY, Hosseini F, Chen H, Sathiyaraj T, Hassanabadi H. A New Approach for Calculation of Quasi-Normal Modes and Topological Charges of Regular Black Holes. arXiv preprint [arXiv:2408.04704](https://arxiv.org/abs/2408.04704). 2024 Aug 8.
- [54] Yasir M, Tiecheng X, Jawad A. Topological charges via Barrow entropy of black hole in metric-affine gravity. *The European Physical Journal C*. 2024 Sep;84(9):1-5.
- [55] Wu SP, Wei SW. Thermodynamical topology of quantum BTZ black hole. *Physical Review D*. 2024 Jul 15;110(2):024054.
- [56] Tong CW, Wang BH, Sun JR. Topology of black hole thermodynamics via Rényi statistics. *The European Physical Journal C*. 2024 Aug 17;84(8):826.
- [57] Mehmood A, Alessa N, Shahzad MU, Zotos EE. Davies-type phase transitions in 4D Dyonic AdS black holes from topological perspective. *Nuclear Physics B*. 2024 Sep 1;1006:116653.
- [58] Bhattacharya K, Bamba K, Singleton D. Topological interpretation of extremal and Davies-type phase transitions of black holes. *Physics Letters B*. 2024 Jul 1;854:138722.
- [59] Hazarika B, Gogoi NJ, Phukon P. Revisiting thermodynamic topology of Hawking-Page and Davies type phase transitions. *Journal of High Energy Astrophysics*. 2025 Mar 1;45:87-95.
- [60] Chen WX. Thermodynamic Topology of Quantum RN Black Holes. arXiv preprint [arXiv:2405.04541](https://arxiv.org/abs/2405.04541). 2024 Apr 25.
- [61] He Y, Lei C, Chen D. Topological Thermodynamics in the Five-Dimensional Gauged Supergravity. Available at SSRN 4725538.
- [62] Obregón, O. Superstatistics and Gravitation. *Entropy* 2010, 12, 2067-2076. <https://doi.org/10.3390/e12092067>
- [63] Ourabah K, Barboza Jr EM, Abreu EM, Neto JA. Superstatistics: Consequences on gravitation and cosmology. *Physical Review D*. 2019 Nov 15;100(10):103516.
- [64] Cai RG. Gauss-Bonnet black holes in AdS spaces. *Physical Review D*. 2002 Mar 25;65(8):084014.
- [65] Yerra PK, Bhamidipati C. Topology of black hole thermodynamics in Gauss-Bonnet gravity. *Physical Review D*. 2022 May 15;105(10):104053.
- [66] Qu Y, Tao J, Yang H. Thermodynamics and phase transition in central charge criticality of charged Gauss-Bonnet AdS black holes. *Nuclear Physics B*. 2023 Jul 1;992:116234.
- [67] Li HL, Zeng XX, Lin R. Holographic phase transition from novel Gauss-Bonnet AdS black holes. *The European Physical Journal C*. 2020 Jul;80(7):652.
- [68] Gubser SS, Klebanov IR, Polyakov AM. Gauge theory correlators from non-critical string theory. *Physics Letters B*. 1998 May 28;428(1-2):105-14.
- [69] Witten E. Anti de Sitter space and holography. arXiv preprint [hep-th/9802150](https://arxiv.org/abs/hep-th/9802150). 1998 Feb 20.



- [70] Ahmed MB, Cong W, Kubizňák D, Mann RB, Visser MR. Holographic dual of extended black hole thermodynamics. *Physical Review Letters*. 2023 May 5;130(18):181401.
- [71] Visser MR. Holographic thermodynamics requires a chemical potential for color. *Physical Review D*. 2022 May 15;105(10):106014.
- [72] Cong W, Kubizňák D, Mann RB, Visser MR. Holographic CFT phase transitions and criticality for charged AdS black holes. *Journal of High Energy Physics*. 2022 Aug;2022(8):1-37.
- [73] Sadeghi J, Alipour MR, Afshar MA, Noori Gashti S. Exploring the phase transition in charged Gauss–Bonnet black holes: a holographic thermodynamics perspectives. *General Relativity and Gravitation*. 2024 Aug;56(8):93.
- [74] Anand A, Gashti SN. Universal Relations with the Non-Extensive Entropy Perspective. *arXiv preprint [arXiv:2411.02875](https://arxiv.org/abs/2411.02875)*. 2024 Nov 5.
- [75] Rani S, Jawad A, Moradpour H, Tanveer A. Tsallis entropy inspires geometric thermodynamics of specific black hole. *The European Physical Journal C*. 2022 Aug 16;82(8):713.
- [76] Rani S, Jawad A, Hussain M. Impact of barrow entropy on geometrothermodynamics of specific black holes. *The European Physical Journal C*. 2023 Aug 9;83(8):710.
- [77] Crossley, Michael, Ethan Dyer, and Julian Sonner. "Super-Rényi entropy & Wilson loops for  $\mathcal{N} = 4$  SYM and their gravity duals." *Journal of High Energy Physics* 2014.12 (2014): 1-25.
- [78] Promsiri C, Hirunsirisawat E, Liewrian W. Thermodynamics and Van der Waals phase transition of charged black holes in flat spacetime via Rényi statistics. *Physical Review D*. 2020 Sep 15;102(6):064014.
- [79] Rényi A. On the dimension and entropy of probability distributions. *Acta Mathematica Academiae Scientiarum Hungarica*. 1959 Mar;10:193-215.
- [80] Barzi F, El Moumni H, Masmar K. Rényi topology of charged-flat black hole: Hawking-Page and Van-der-Waals phase transitions. *Journal of High Energy Astrophysics*. 2024 Jun 1;42:63-86.
- [81] Masi M. A step beyond Tsallis and Rényi entropies. *Physics Letters A*. 2005 May 2;338(3-5):217-24.
- [82] Majhi A. Non-extensive statistical mechanics and black hole entropy from quantum geometry. *Physics Letters B*. 2017 Dec 10;775:32-6.
- [83] Jahromi AS, Moosavi SA, Moradpour H, Graça JM, Lobo IP, Salako IG, Jawad A. Generalized entropy formalism and a new holographic dark energy model. *Physics Letters B*. 2018 May 10;780:21-4.
- [84] Majhi A. Non-extensive statistical mechanics and black hole entropy from quantum geometry. *Physics Letters B*. 2017 Dec 10;775:32-6.
- [85] Mejrhit K, Ennadifi SE. Thermodynamics, stability and Hawking–Page transition of black holes from non-extensive statistical mechanics in quantum geometry. *Physics Letters B*. 2019 Jul 10;794:45-9.
- [86] Liu Y. Non-extensive statistical mechanics and the thermodynamic stability of FRW universe. *Europhysics Letters*. 2022 May 24;138(3):39001.
- [87] Veraguth OJ, Wang CH. Immirzi parameter without Immirzi ambiguity: Conformal loop quantization of scalar-tensor gravity. *Physical Review D*. 2017 Oct 15;96(8):084011.
- [88] Wang CH, Rodrigues DP. Closing the gaps in quantum space and time: Conformally augmented gauge structure of gravitation. *Physical Review D*. 2018 Dec 15;98(12):124041.
- [89] Wang CH, Stankiewicz M. Quantization of time and the big bang via scale-invariant loop gravity. *Physics Letters B*. 2020 Jan 10;800:135106.
- [90] Nojiri SI, Odintsov SD, Faraoni V. From nonextensive statistics and black hole entropy to the holographic dark universe. *Physical Review D*. 2022 Feb 15;105(4):044042.